Journal of Alloys and Compounds 506 (2010) 888–891

Contents lists available at ScienceDirect

Journal of Alloys and Compounds

journal homepage: www.elsevier.com/locate/jallcom

Synthesis of $LiNi_{0.65}Co_{0.25}Mn_{0.1}O_2$ as cathode material for lithium-ion batteries by rheological phase method

Cuixia Cheng[a], Long Tan[b], Anzheng Hu[a], Haowen Liu[b,*], Xintang Huang[a,**]

[a] Center of Nano-Science and Technology, Department of Physics, Central China Normal University, Wuhan 430079, PR China
[b] Key Laboratory of Catalysis and Materials Science of the State Ethnic Affairs Commission & Ministry of Education, Hubei Province, South-Central University for Nationalities, Wuhan, 430074, PR China

ARTICLE INFO

Article history:
Received 12 April 2010
Received in revised form 13 July 2010
Accepted 13 July 2010
Available online 21 July 2010

Keywords:
Lithium-ion batteries
Cathode
$LiNi_{0.65}Co_{0.25}Mn_{0.1}O_2$
Rheological phase method

ABSTRACT

Rheological phase (RP) method has been successfully applied to synthesize a promising cathode material $LiNi_{0.65}Co_{0.25}Mn_{0.1}O_2$. X-ray diffraction, X-ray photoelectron spectroscopy, inductively coupled plasma and transmission electron microscope are used to investigate the structure, composition and morphology, respectively. XRD result shows that the as-prepared powder has a layered α-$NaFeO_2$ structure. XPS pattern reveals that the Ni ions have valences of 2+ and 3+, and the Co and Mn are 3+, 4+, respectively. The electrode consisting of the obtained powder presents the better electrochemical properties, which is attributed to the fewer amounts of Ni^{2+} ions and the smaller particles. All the results suggest that the rheological phase method is a promising technique for the preparation of $LiNi_{0.65}Co_{0.25}Mn_{0.1}O_2$ cathode material of lithium-ion batteries.

1. Introduction

Lithium-ion batteries have been widely applied in hybrid electric vehicle (HEV), laptop, mobile phone, and other. The earliest and dominant commercial cathode material applied in lithium-ion batteries is $LiCoO_2$ [1,2]. However, the following drawbacks impede its development: (i) Co is expensive and toxic. (ii) Extracting more Li-ions from $Li_{0.5}CoO_2$ (by raising the charge cut-off voltage over 4.2 V) leads to a decrease in the lattice constant *c* via a transition from the hexagonal to the monoclinic phase, and thereby collapses the structure. With increasing market demand, it is necessary to search for a new cathode material of the lower cost, lower toxicity and also ease of preparation to replace $LiCoO_2$ [3,4].

$LiNiO_2$ has the higher specific capacity and is cheaper than $LiCoO_2$, but it is both electrochemically and chemically unstable, leading to both synthesis and safety problems [5]. One approach to improve the electrochemical performance is to partially substitute manganese cobalt nickel oxides. It has been identified that $LiNi_xCo_yMn_{(1-x-y)}O_2$, a combination of cathode cations Ni, Co, and Mn has been reported as a promising positive material for rechargeable Li-ion batteries [6–8]. These materials belong to α-$NaFeO_2$ type. The valences of nickel, cobalt, and manganese ions are 2+, 3+, and 4+, respectively, and only nickel ions and cobalt ions are electro-active. It is reported that even 200 mAh g^{-1} can be attainable when charged up to 4.6 V [9]. However, it is usually synthesized by a long sintering time. As for $LiNi_{0.65}Co_{0.25}Mn_{0.1}O_2$, a material which has been first synthesized and investigated by Saadoune et al. via combustion method [10], can be prepared with less time compared to $LiNi_{1/3}Co_{1/3}Mn_{1/3}O_2$ [9]. Furthermore, $LiNi_{0.65}Co_{0.25}Mn_{0.1}O_2$ has the higher productivity and the lower cost, which makes it fascinating for the battery manufacturers.

It is well known that synthesis method plays an important role in affecting the electrochemical properties of material. Recently, rheological phase reaction method, a simple and effective route, uses chelation reagent to enable molecular level mixing of different reactants, and thus leads to a homogeneous structure of the final product. This method can effectively improve the electrochemical properties in our previous study [11]. In this paper, rheological phase reaction method is used to synthesize a promising cathode $LiNi_{0.65}Co_{0.25}Mn_{0.1}O_2$ of lithium-ion batteries. Its structure, composition and electrochemical properties have also been investigated.

2. Experiment details

$LiNi_{0.65}Co_{0.25}Mn_{0.1}O_2$ has been prepared using NiO, Co_3O_4, MnO_2 and $LiOH{\cdot}H_2O$ as the raw reaction materials. Stoichiometric NiO, Co_3O_4, MnO_2, $LiOH{\cdot}H_2O$ and

* Corresponding author at: Key Laboratory of Catalysis and Materials Science of the State Ethnic Affairs Commission & Ministry of Education, Hubei Province, South-Central University for Nationalities, Wuhan, 430074, PR China.
Tel.: +86 27 6784 2752; fax: +86 27 6784 2752.
** Corresponding author at: Center of Nano-Science and Technology, Department of Physics, Central China Normal University, Wuhan 430079, PR China.
Tel.: +86 27 6786 7004; fax: +86 27 6786 1185.
E-mail addresses: liuhwchem@mail.scuec.edu.cn (H. Liu), xthuang@phy.ccnu.edu.cn (X. Huang).

0925-8388/$ – see front matter. Crown Copyright © 2010 Published by Elsevier B.V. All rights reserved.
doi:10.1016/j.jallcom.2010.07.105

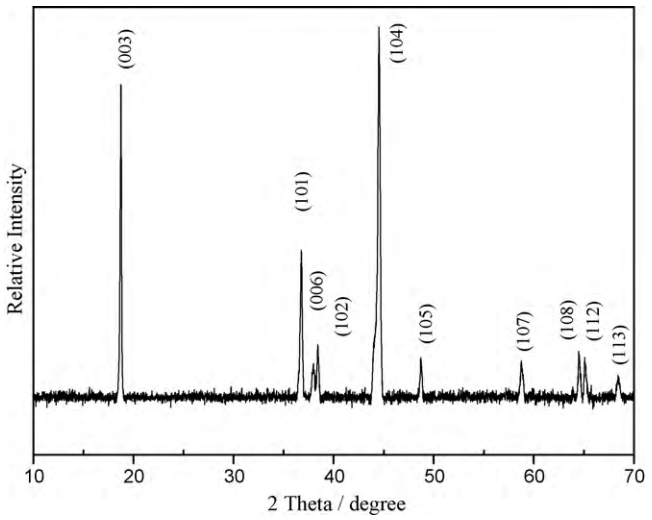

Fig. 1. X-ray diffraction pattern of the as-prepared powder.

appropriate amount of citric acid are roughly mixed in an agate mortar. Then, proper quantity of distilled water (0.01% of the total mass) is added to form rheological phase mixture which is reacted in an oven at 150 °C for 6 h. An obtained precursor is calcined at 500 °C and 900 °C for 3 h, respectively.

All the reagents used in experiment are of analytical purity and have been purchased from Shanghai Chemical Reagent Company and used without further purification. The crystalline phase was analyzed using X-ray diffraction (XRD, Bruker D8-advance, Germany) with Cu Kα radiation. The XRD data was collected with 0.02° step size in the range of $10° \leq 2\theta \leq 70°$ with a constant counting time of 0.1 s per step at 40 kV and 40 mA. X-ray photoelectron spectroscopy (XPS) was performed with Thermo VG Multi Lab2000 America with a Mono Al Kα light source (300 W). The synthesis powder was mounted on a XPS stage using conductive carbon adhesive tape. Each spectrum is calibrated using the C 1s binding energy at 284.6 eV. The chemical composition of the as-synthesized sample was checked by inductively coupled plasma (ICP) with atomic emission spectroscopy (ICP-AES, model IRIS, TJA, USA). The morphology was observed with a transmission electron microscope (TEM, FEI, TECNAI G220 S-Twin, America). The electrochemical impedance spectroscopy (EIS) was carried out on the same cell as the cycling experiment by applying an ac voltage of 10 mV over the frequency range from 1 Hz to 100 kHz (BAS, EG and Ginstrument). The simulate cells were assembled by using lithium foil as anode in an argon-filled glove box, the prepared powder mixed with 12% acetylene black and 8% polytetrafluoroethylene (PTFE) as the cathode and 1 M $LiPF_6$ in a 1:1 (v/v) mixture of ethylene carbonate (EC) and dimethylcarbonate (DMC) as the electrolyte, Celgard 2300 membrane as the cell separator. The charge–discharge cycles have been performed at a serial of current densities ($1\,C = 0.8\,mA\,cm^{-2}$) in the voltage of 2.5–4.5 V using the simulate cells. All the electrical measurements were carried out by a battery testing system (RFT-5 V/10 mA, corporation of Luhua electronic equipment, China) at room temperature.

3. Results and discussion

3.1. Property of structure

The XRD pattern of the as-synthesized powder is shown in Fig. 1. All the diffraction peaks can be identified as a typical $NaFeO_2$ structure with space group $R\bar{3}m$, which indicates that the obtained sample with a predicted layered crystal structure is pure phase. Additionally, the peaks are obviously sharper, and the split of 0 0 6/1 0 2, 1 0 8/1 1 0 doublet can be clearly seen, which could be regarded as the characteristic of the layered structure materials [12]. In our case, the 0 0 6/1 0 2 and 1 0 8/1 1 0 peaks are clearly separated, indicating the formation of highly ordered layered structure. It is expected that the higher ordered structure would lead to the better electrochemical performances. The refinement was terminated by tops R software, and the lattice parameters obtained from Rietveld refinement with a convincible R_{wp} value (3.049) is $a = 1.5154$ Å, $c = 15.192$ Å. It is important to note that the a value is less than that of the report [10], which may due to the increase of Ni^{3+} ions and lead to the better electrochemical properties.Study on the compositions and valences of elementsICP and XPS were used to investigate the composition of the obtained powder. A ratio of Li/Ni/Co/Mn determined by ICP is 9.8:6.5:2.4:0.9, which was close to the theoretical value (1:0.65:0.25:0.1). As shown in the XPS sur-

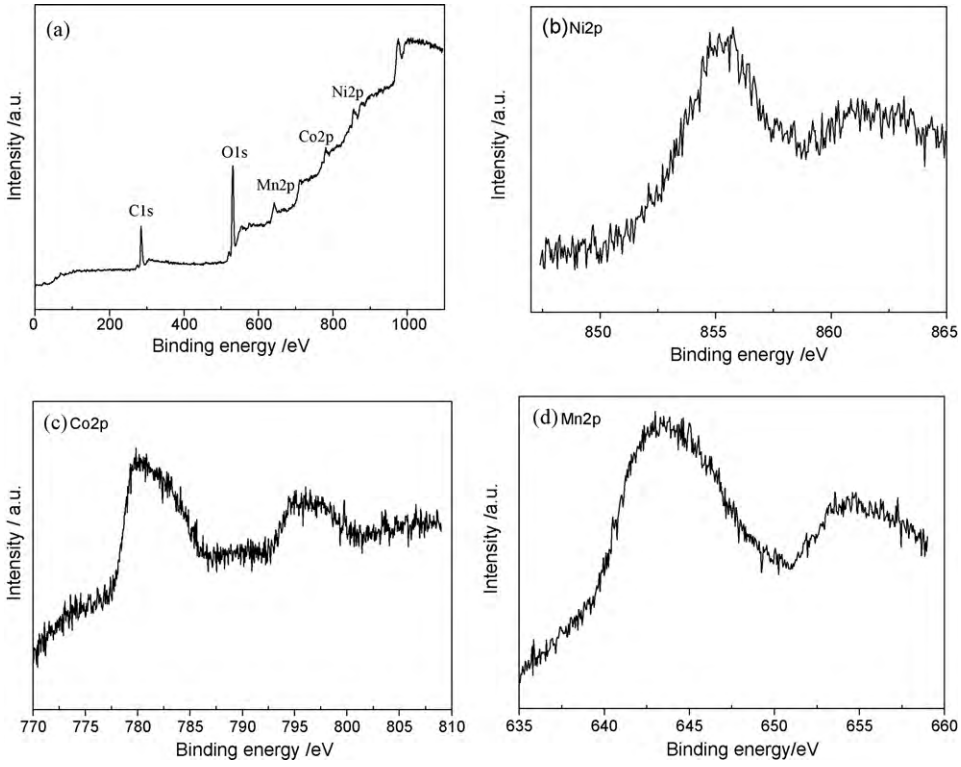

Fig. 2. X-ray photoelectron spectroscopy pattern of the as-synthesized $LiNi_{0.65}Co_{0.25}Mn_{0.1}O_2$: (a) survey spectrum (b) high-resolution spectra of Ni (c) high-resolution spectra of Co (d) high-resolution spectra of Mn.

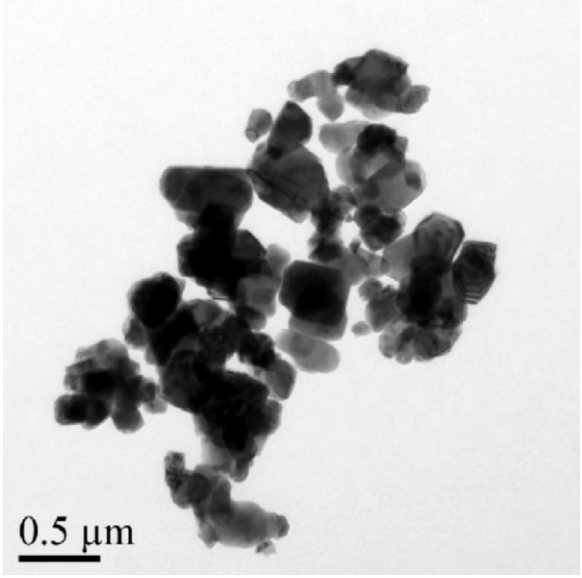

Fig. 3. TEM image of the as-synthesized $LiNi_{0.65}Co_{0.25}Mn_{0.1}O_2$.

vey spectrum (Fig. 2a), this sample consists of Ni, Co, Mn, O and C elements. In the high-resolution spectra (Fig. 2b–d), the Mn2p binding energy of the powder is located at 642.8 eV and the Co2p binding energy is 779.8 eV, which matches well with the values reported by Li et al. [13]. It indicates that the oxidation states of the Mn and Co are 4+ and 3+, respectively. A typical satellite peak around 861 eV is also noted in addition to the Ni2p3/2 peak. Such a satellite peak is also observed in NiO, $LiNiO_2$ and $LiMn_{1.5}Ni_{0.5}O_4$. It is attributed to the multiple splitting in the energy level of the Ni-containing oxides [14]. The Ni2p3/2 spectrum is fitted to two peaks with binding energy values of 854.4 eV and 855.9 eV, which corresponds to Ni^{2+} and Ni^{3+}, respectively. It has been reported that the existence of both Ni^{2+} and Ni^{3+} are beneficial for the electronic conductivity of the material [15].

3.3. TEM analysis

An image of the obtained powder is observed by TEM and displayed in Fig. 3. It can be clearly seen that the RP sample has well-dispersed submicron particles with irregular shape. The average size for this RP sample is about 0.3 μm. It is obvious that the smaller and well-dispersed particles of RP should be attributed to the effect of citric acid as a dispersant in the calcination step.

3.4. Electrochemical properties

The charge–discharge experiments of the obtained sample were carried out in the voltage of 2.5–4.5 V. The constant current densities are 0.125, 0.25 and 0.375 C, respectively. As seen in Fig. 4, the initial discharge curves in various current densities are 130.5 mAh g^{-1} (0.125 C), 123.4 mAh g^{-1} (0.25 C), 114.6 mAh g^{-1} (0.375 C). The similar $LiNi_{0.65}Co_{0.25}Mn_{0.1}O_2$ positive electrode material presents 140 mAh g^{-1} discharge capacity at 0.05 C [10]. The obtained different discharge capacity may be attributed to different voltage range, charge–discharge current density, the particle size and the Ni^{2+} quantity in the powder. The bigger voltage range, the higher rate, the bigger size and the amount of extra Ni^{2+} lead to the lower capacity, which is a classical phenomenon in Li-ion batteries [10,16]. Fig. 5 shows that the discharge capacities are retained during 20 cycles at different current densities in 2.5–4.5 V. The discharge capacity loss is equal to 3.1%, 18.5% and 36.9% after 20 cycles at 0.125, 0.25 and 0.375 C, respectively. However, the better discharge capacity loss is 16% after 20 cycles at 0.05 C [10]. The electrodes consisting of RP powder exhibit superior rate capabilities, which could be attributed to the less a value and the smaller particles. The less a value shows the decrease of the Li^+/Ni^{2+} cation mixing and leads to the improvement of electrochemical properties. Furthermore, the smaller size can decrease the distance of diffusion for Li-ions in the host, thereby improving the rate capability. In other hand, the smaller particle has the lager surface area. This makes the addition of conductive additives to the active material easier. It is helpful to lower the cell polarization and improve the reversible capacity [10].

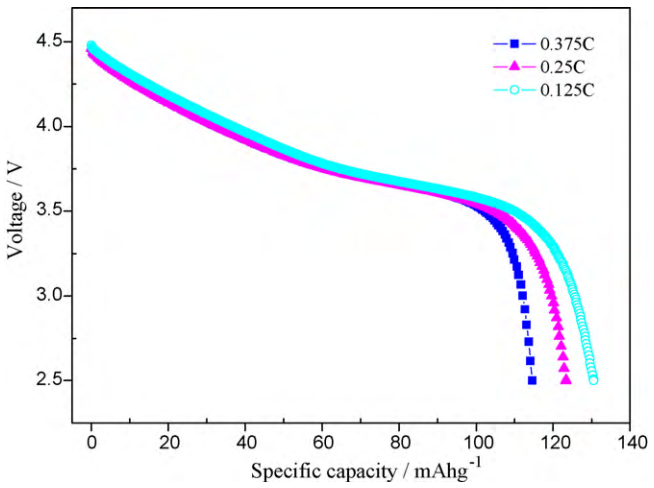

Fig. 4. The initial discharged curves for the as-prepared $LiNi_{0.65}Co_{0.25}Mn_{0.1}O_2$ at different current in 2.5–4.5 V.

In order to further elucidate the electrochemical properties of the RP powder, EIS analysis of the composite electrode have been carried out, and the results are shown in Fig. 6. A semicircle is observed in the high frequency domain, and its origin has been ascribed to the lithium-ion migration through the interface between the surface layer of the particles and the electrolyte [17,18]. The calculated surface layer resistance is 70 Ω. After charge–discharged at 0.25 C for one cycle, the surface layer resistance increases by 110 Ω. It has been reported that the increase of resistance is both related to the solid electrode interface (SEI) film on the $LiNi_{0.65}Co_{0.25}Mn_{0.1}O_2$ and cathode ability to accept lithium-ions during the first discharge [19]. After the first, second and fifth cycle, the cathode materials adhered to the Celgard 2300 mem-

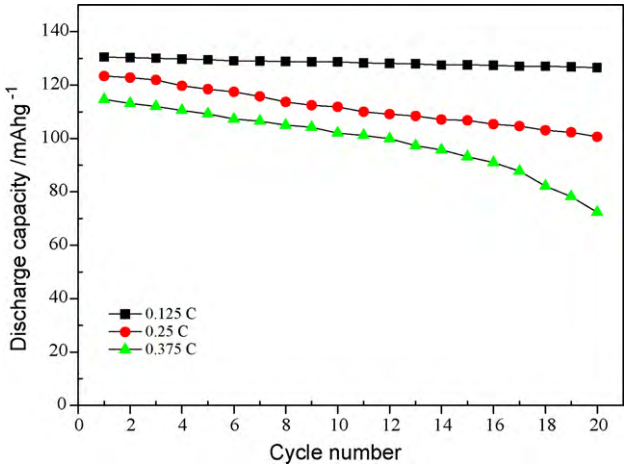

Fig. 5. Variation of discharge capacity vs number of cycles using the as-prepared $LiNi_{0.65}Co_{0.25}Mn_{0.1}O_2$ as cathode material at different current between 2.5 and 4.5 V.

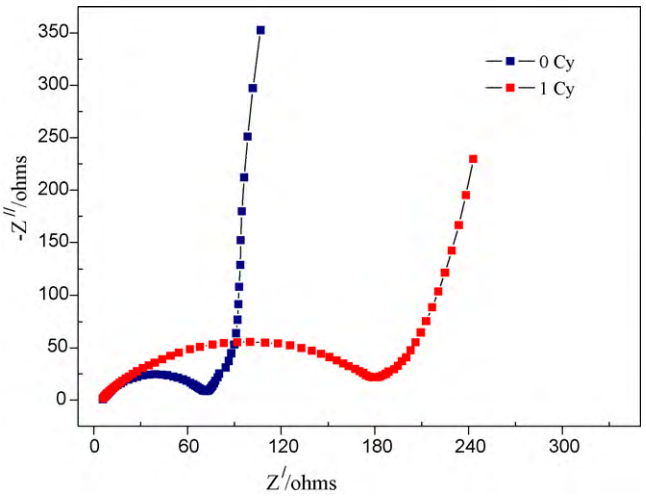

Fig. 6. Electrochemical impedance spectroscopy analysis of the as-prepared $LiNi_{0.65}Co_{0.25}Mn_{0.1}O_2$: (0 Cy) before charge–discharge test, (1 Cy) after one charge–discharge test.

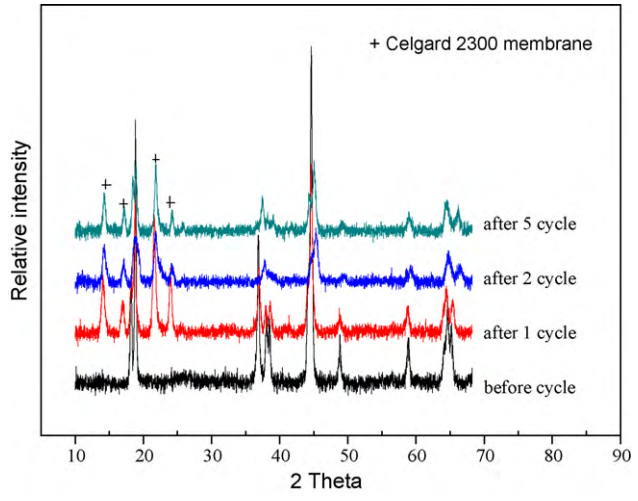

Fig. 7. X-ray diffraction patterns of the electrode $LiNi_{0.65}Co_{0.25}Mn_{0.1}O_2$ before charge–discharge and after charge–discharge.

brane were taken out from the simulate cells and kept for 12 h at 100 °C, then was measured by XRD analysis. The results are shown in Fig. 7. Compared to that of the electrode material before cycle, the curves are nearly similar shape except for some impurity peaks detected as the Celgard 2300 membrane, which indicates that the layer structure of $LiNi_{0.65}Co_{0.25}Mn_{0.1}O_2$ prepared by RP is very stable and the insertion and extraction of lithium-ions occurred reversibly during charge–discharge process. This stabilizing structure can also effectively restrain concentration polarization and helpful for lithium-ions diffusion. Another difference is that some broadening peaks can be seen, which may indicate microstructural defects or a nonuniform distribution of local strain do exist [20]. The further study aimed at clarifying this phenomenon is in progress.

4. Conclusions

$LiNi_{0.65}Co_{0.25}Mn_{0.1}O_2$ with layered $NaFeO_2$ structure has been successfully synthesized by rheological phase method. XRD and TEM data indicate the obtained powder is better crystallized and the smaller size. Charge–discharge test results show that the RP powder presents the better electrochemical properties in the voltage region of 2.5–4.5 V, which is due to the smaller particles and the lower Ni^{2+} quantity in the powder. In additional, the surface layer resistance for the as-prepared powder is only about 70 Ω, which is convenient for inserting and deinserting of lithium-ions from the $LiNi_{0.65}Co_{0.25}Mn_{0.1}O_2$ powder prepared by rheological phase method.

Acknowledgment

The authors gratefully acknowledge the financial support from the National Natural Science Foundation of China (No. 50872039).

References

[1] C. Zhu, C. Yang, W. Yang, C. Hsieh, H. Ysai, Y. Chen, J. Alloys Compd. 496 (2010) 703–709.
[2] J. Shu, M. Shui, F. Huang, Y. Ren, Q. Wang, D. Xu, L. Hou, J. Phys. Chem. C 114 (2010) 3323–3328.
[3] Y. Lin, M.X. Gao, D. Zhu, Y.F. Liu, H.G. Pan, J. Power Sources 184 (2008) 444–448.
[4] M. Gao, Y. Lin, Y. Yin, Y. Liu, H. Pan, Electrochim. Acta (2010), doi:10.1016/j.electacta.2010.02.003.
[5] S. Sivaprakash, S.B. Majumder, J. Alloys Compd. 479 (2009) 561–568.
[6] H. Kobayashi, Y. Arachi, S. Emura, H. Kageyama, K. Tatsumi, T. Kamiyama, J. Power Sources 146 (2005) 640–644.
[7] K. Du, Z. Peng, G. Hu, Y. Yang, L. Qi, J. Alloys Compd. 476 (2009) 329–334.
[8] H. Xia, H. Wang, W. Xiao, L. Lu, M.O. Lai, J. Alloys Compd. 48 (2009) 696–701.
[9] C.H. Lu, B.J. Shen, J. Alloys Compd. 497 (2010) 159–165.
[10] I. Saadoune, M. Dahbi, M. Wikberg, T. Gustafsson, P. Svedlindh, K. Edström, Solid State Ionics 178 (2008) 1668–1675.
[11] L. Tan, Z. Luo, H. Liu, Y. Yu, J. Alloys Compd. 502 (2010) 407–410.
[12] Y.S. He, L. Pei, X.Z. Liao, Z.F. Ma, J. Fluorine Chem. 128 (2007) 139–143.
[13] X. Li, Y.J. Wei, H. Ehrenberg, F. Du, C.Z. Wang, G. Chen, Solid State Ionics 178 (2008) 1969–1974.
[14] K.M. Shaju, G.V. Subba Rao, B.V.R. Chowdari, Electrochim. Acta 48 (2002) 145–151.
[15] D. Li, Y. Sasaki, M. Kageyama, K. Kobayakawa, Y. Sato, J. Power Sources 148 (2005) 85–89.
[16] H. Liu, H. Yang, J. Li, Electrochim. Acta 55 (2010) 1626–1629.
[17] D. Li, Y. Kato, K. Kobayakawa, H. Noguchi, Y. Sato, J. Power Sources 160 (2006) 1342–1348.
[18] R. Guo, P. Shi, X. Cheng, C. Du, J. Alloys Compd. 473 (2008) 53–59.
[19] S.H. Kang, D.P. Abraham, W.S. Yoon, K.W. Nam, X.Q. Yang, Electrochim. Acta 54 (2008) 684–689.
[20] J. Tu, X.B. Zhao, G.S. Cao, J.P. Tu, T.J. Zhu, J. Mater. Lett. 60 (2006) 3251–3254.